

# Pronounced electromigration of Cu in molten Sn-based solders

J.R. Huang and C.M. Tsai

*Department of Chemical & Materials Engineering, National Central University, Zhongli City, Taiwan*

Y.W. Lin and C.R. Kao<sup>a)</sup>

*Department of Materials Science & Engineering, National Taiwan University, Taipei City 106, Taiwan*

(Received 25 July 2007; accepted 5 October 2007)

The high local temperature in flip-chip solder joints of microprocessors has raised concerns that the solder, a low melting temperature alloy, might locally liquefy and consequently cause failure of the microprocessors. This article reports a highly interesting electromigration behavior when the solder is in the molten state. A  $6.3 \times 10^3$  A/cm<sup>2</sup> electron current was applied to molten Sn3.5Ag solder at 255 °C through two Cu electrodes. The high current density caused rapid dissolution of the Cu cathode. The dissolved Cu atoms were driven by electrons to the anode side and precipitated out as a thick, and sometimes continuous, layer of Cu<sub>6</sub>Sn<sub>5</sub>. The applied current caused the dissolution rate of the Cu cathode to increase by one order of magnitude. A major difference between the electromigration in the solid and molten state was identified to be the presence of different countering fluxes in response to electromigration. For electromigration in the molten state, the back-stress flux, which was operative for electromigration in the solid state, was missing, and instead a countering flux due to the chemical potential gradient was present. An equation for the chemical potential gradient,  $d\mu/dx$ , required to balance the electromigration flux was derived to be  $d\mu/dx = N^{\circ}z^*e\rho J$ , where  $N^{\circ}$  is Avogadro's number,  $z^*$  is the effective charge of Cu,  $e$  is the charge of an electron,  $\rho$  is the resistivity of the solder, and  $J$  is the electron current density.

## I. INTRODUCTION

To meet the demand for decreasing packaging size, the electron current density through the flip-chip solder joints of microprocessors has to increase with every new generation of devices. It is anticipated the current density through flip-chip solder joints will soon reach  $10^4$  A/cm<sup>2</sup>.<sup>1</sup> At such a current density level, two concurrent processes, electromigration and Joule heating, present challenging materials problems.<sup>2</sup> Several failure mechanisms have been reported for flip-chip solder joints under the stressing of high current density. In the void formation-and-propagation mechanism,<sup>3,4</sup> a void first initiates at the current density crowding region. It then extends along the under bump metallurgy (UBM)/solder interface, and eventually forms a gap between the UBM and

the solder, resulting in an open circuit failure. The main process responsible for this mechanism is electromigration. Joule heating plays a secondary role in raising the local temperature. Nevertheless, Joule heating can play a more dominating role under certain conditions. Recently, the local melting of the solder induced by Joule heating was identified as an operative failure mechanism.<sup>5,6</sup> Moreover, Alam et al.<sup>6</sup> pointed out the rapid Cu dissolution reported in the literature<sup>7-9</sup> was in fact caused by the contact of the Cu UBM with the molten solder. Because under certain conditions solder can become molten during current stressing, the knowledge of electromigration behaviors in molten solder alloys becomes important.

The objective of this study is to examine Cu electromigration in molten Sn3.5Ag (wt%) solder, which is an important lead-free solder alloy. For comparison, electromigration in the solid state is also performed for the same system at the same current density.

## II. EXPERIMENTAL

The configuration of the current stressing experiment is shown in Fig. 1. A capillary tube with a 450- $\mu$ m inside

<sup>a)</sup>Address all correspondence to this author.

e-mail: crkao@ntu.edu.tw

This author was an editor of this journal during the review and decision stage. For the *JMR* policy on review and publication of manuscripts authored by editors, please refer to [http://www.mrs.org/jmr\\_policy](http://www.mrs.org/jmr_policy).

DOI: 10.1557/JMR.2008.0024

diameter was filled with Sn3.5Ag solder, and Cu wires (420- $\mu\text{m}$  diameter) were then inserted into the two ends of the capillary tube. The separation between the two ends of the two Cu wires was maintained at 500  $\mu\text{m}$ . Before each Cu wire was inserted, an indent was created on the Cu wire by a hardness tester to serve as a marker for monitoring the consumed thickness of the Cu wire during the experiment. As shown in Fig. 1, the electrons entered the molten solder from the Cu wire on the left side (cathode), passed through the molten solder, and exited through the Cu wire on the right side (anode). The applied current was 10 A, producing an average current density of  $6.3 \times 10^3 \text{ A/cm}^2$  in the solder.

The experiment was carried out in an oven set at 240  $^\circ\text{C}$ . Because of Joule heating, the temperature of the molten solder and the Cu electrodes rose from 240  $^\circ\text{C}$  to a steady-state temperature of 255  $^\circ\text{C}$  in 30 s after the current was applied. Therefore, the results in this study should be considered to have been obtained at 255  $^\circ\text{C}$ .

To compare behavior with the solid-state solder, the same experiment was also conducted in an oven set at 185  $^\circ\text{C}$ . Because of Joule heating, the temperature of the solder and the Cu electrodes rose to a steady-state temperature of 200  $^\circ\text{C}$ , at which Sn3.5Ag remained in the solid state.

### III. RESULTS

#### A. Electromigration in molten Sn3.5Ag

The sample after assembly but before the current stressing is shown in Figs. 2(a) and 2(b). The Cu/solder interfaces on both sides were sharp, and there was a very small amount of intermetallic, presumably  $\text{Cu}_6\text{Sn}_5$ , near both interfaces.

The sequence of events during current stressing at 255  $^\circ\text{C}$  is shown in Figs. 3(a)–3(d). After 30 min of current stressing, as shown in Fig. 3(a), a large amount of intermetallic compound (IMC) formed in the solder near the anode side. Electron microprobe analysis revealed the compound was  $\text{Cu}_6\text{Sn}_5$ . The compound at this stage displayed rod morphology, radiating from the solder/anode interface into the solder with different take-off angles. The surface plane of the micrograph of Fig. 3(a) cuts through these  $\text{Cu}_6\text{Sn}_5$  rods at different angles, revealing different cross-sections of these rods. Lu et al.<sup>10</sup> recently published an excellent article relating the cross-sectional morphology of such  $\text{Cu}_6\text{Sn}_5$  rods to their real three-dimensional microstructure.

Accompanying the formation of  $\text{Cu}_6\text{Sn}_5$  was the rapid dissolution of the Cu cathode. As shown in Fig. 4, 50  $\mu\text{m}$  of the Cu cathode had been dissolved after just 30 min of current stressing. The dissolved Cu atoms from the cathode were driven by electromigration to the anode side and precipitated out as  $\text{Cu}_6\text{Sn}_5$ .

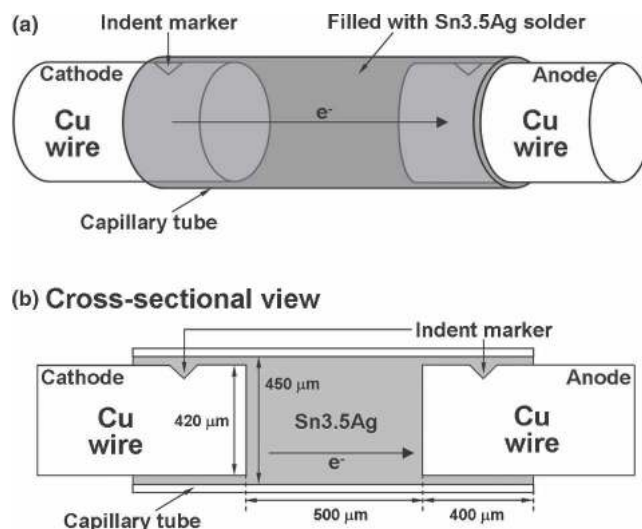


FIG. 1. Schematic drawing showing the configuration of the current-stressing experiment (a) in stereoview and (b) in cross-sectional view. Current density through the molten solder was  $6.3 \times 10^3 \text{ A/cm}^2$ , and the molten solder temperature during current stressing was 255  $^\circ\text{C}$ . Electrons entered the molten solder from the Cu wire on the left side (cathode) and exited through the Cu wire on the right side (anode). Indents on the Cu wires were created using a hardness tester and serve as markers for monitoring the consumed thickness of the Cu wires during the experiment.

When the current stressing time reached 60 min, as shown in Figs. 3(b) and 4, more Cu was dissolved, and more  $\text{Cu}_6\text{Sn}_5$  formed near the anode side. As can be seen in Figs. 3(a) and 3(b), the dissolution rate of the Cu

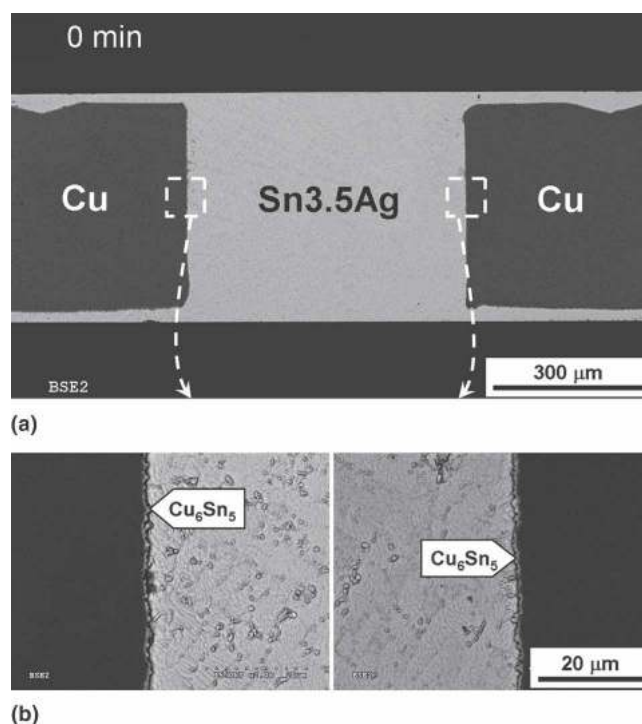


FIG. 2. (a) Micrograph showing the as-assembled sample before current stressing. (b) Zoom-in micrographs showing the two interfaces in (a).

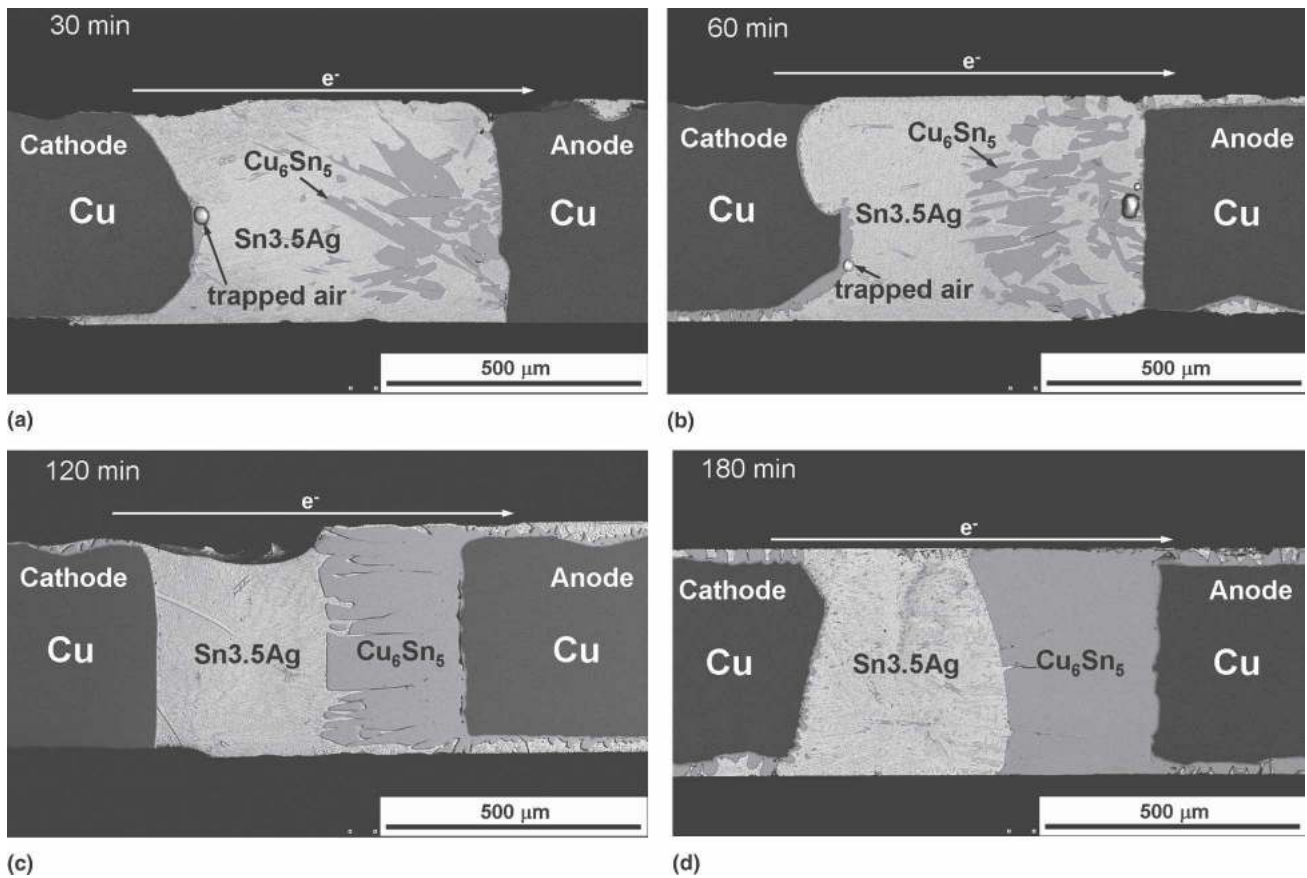


FIG. 3. Micrographs showing the sequence of events during current stressing at 255 °C. The current density through the molten solder was  $6.3 \times 10^3 \text{ A/cm}^2$ , and the electrons flowed from the left side to the right: (a) after 30 min, (b) 60 min, (c) 120 min, and (d) 180 min of current stressing.

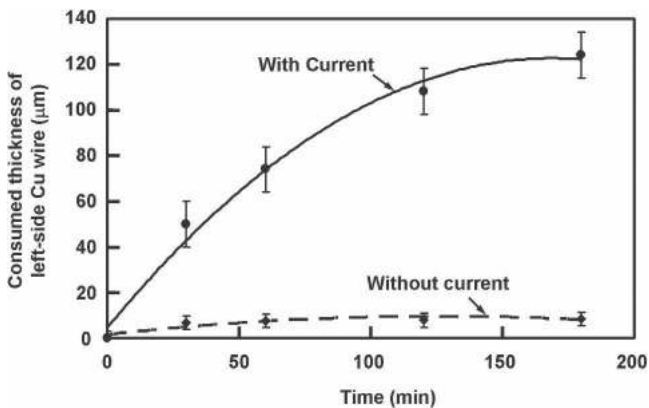


FIG. 4. Consumed thickness of the Cu cathode versus time. Also shown is the consumed thickness for each of the Cu wires at 255 °C for the case of no applied current.

cathode was not homogeneous along the cathode/solder interface. The presence of a trapped air bubble was able to hinder the dissolution of nearby Cu, probably through disrupting the electron flow through that region. When the time reached 120 min and beyond,  $\text{Cu}_6\text{Sn}_5$  no longer had the rod morphology but exhibited the layered morphology, as shown in Figs. 3(c) and 3(d).

To clarify the effect of the electron current, samples were put through the same thermal histories as those of Fig. 3, i.e., at 255 °C for different periods of time, but with no current applied. The effect of electron current can be seen by comparing Fig. 3 with Fig. 5, which shows the no-current samples kept at 255 °C. As can be seen in Fig. 5, only a small amount of  $\text{Cu}_6\text{Sn}_5$  scallops and a thin layer of  $\text{Cu}_3\text{Sn}$  formed at the Cu/solder interfaces on both sides. The microstructure in Fig. 5 is typical of the Cu/solder reaction and has been reported many times in the literature.<sup>11,12</sup> The consumed thickness of each Cu wire for the no-current cases is shown in Fig. 4. As seen in Fig. 4, application of the electron current accelerated Cu consumption by about one order of magnitude.

Figures 3–5 clearly show that the dissolution of the Cu cathode was caused by the applied current because otherwise the Cu dissolution was quite small. Please note that the dissolution of the two Cu electrodes was asymmetrical when a current was applied. Only the dissolution of the Cu cathode was accelerated, and the consumption rate of the Cu anode did not increase. In fact, the consumption rate of the Cu anode was even smaller than the no-current case, and this is not shown in Fig. 4 because it is too small to be measured accurately.



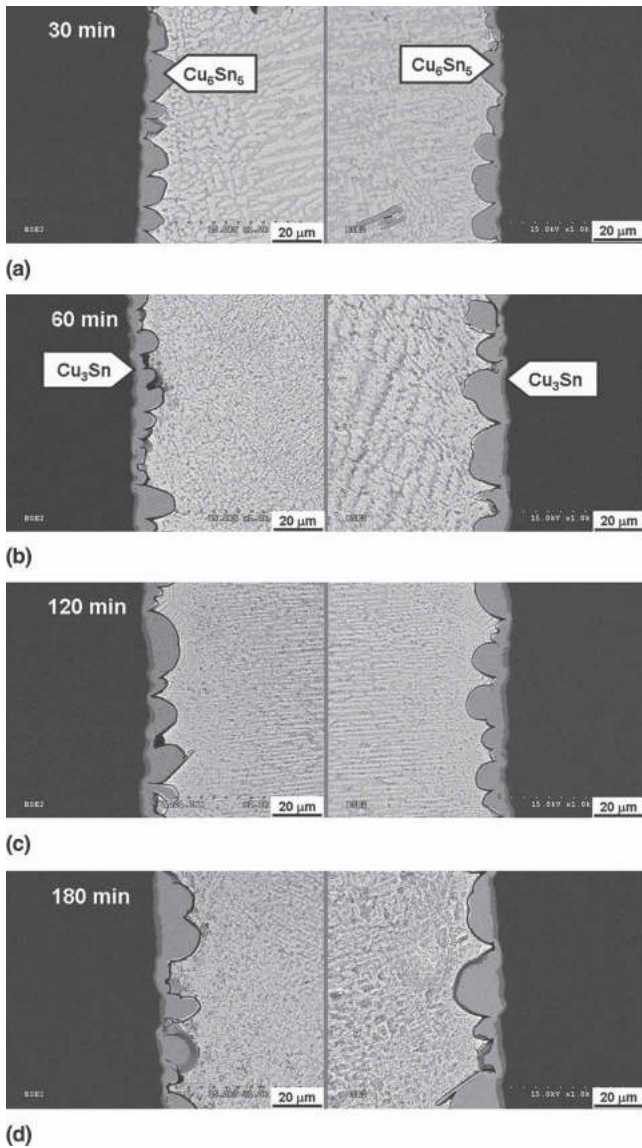


FIG. 5. Micrographs showing the two Cu/solder interfaces at 255 °C when no electron current was applied: (a) after 30 min, (b) 60 min, (c) 120 min, and (d) 180 min.

### B. Electromigration in solid Sn3.5Ag

To compare electromigration in the solid and molten states, the same electromigration experiment was also conducted at 200 °C, which is below the eutectic temperature of Sn3.5Ag (221 °C). Shown in Figs. 6(a)–6(c) are the two Cu/solder interfaces after 180, 2400, and 4000 min of current stressing. Here, an average current density of  $6.3 \times 10^3 \text{ A/cm}^2$  passed through the solder from left to right. Initially, the difference in the total intermetallic thickness at the cathode side and the anode side was not obvious [Fig. 6(a)]. However, after 2400 min there was a clear difference in the thickness [Fig. 6(b)]. The total thickness of the IMCs on the anode side was larger than on the cathode side. Moreover, on

the cathode side a series of voids developed between  $\text{Cu}_6\text{Sn}_5$  and the solder. This series of voids widened as the time reached 4000 min [Fig. 6(c)]. Although the voids in Fig. 6(b) did not stop the electrons from passing through the sample, these voids hindered the interdiffusion between Cu and Sn because the total intermetallic thickness on the cathode side had not increased from 2400 to 4000 min [Fig. 7]. Development of voids on the cathode side under similar experimental conditions was reported by Gan and Tu,<sup>13</sup> who offered excellent explanations and a discussion on the formation of these voids.

Shown in Figs. 8(a)–8(c) is the microstructure evolution when the sample was aged at 200 °C but with no applied electron current. As expected, the growth of the IMCs at the two interfaces was the same. The total thickness plotted versus the aging time is also shown in Fig. 7. It is clear in Fig. 7 that the electron flow enhanced the intermetallic growth on the anode side and reduced the growth on the cathode side. This observation is again consistent with the observations of Gan and Tu.<sup>13</sup>

## IV. DISCUSSION

The most striking feature of electromigration in the molten state is the rapid dissolution of the Cu cathode and the accompanying  $\text{Cu}_6\text{Sn}_5$  formation near the anode (Fig. 3). Two factors, the high current density and the molten state of the conducting media, are identified as critical to bringing about this feature. The results presented in Fig. 5 demonstrate that the molten state alone was not enough to produce the rapid dissolution, and the results in Fig. 6 show that high current density alone was not sufficient, either. In the following, it will be shown the existing literature data can explain this rather interesting phenomenon.

Dybkov described the dissolution kinetics of a substrate into a molten metal by the following equation<sup>14</sup>:

$$\frac{dc}{dt} = k(c_s - c) \quad , \quad (1)$$

where  $c$  is the Cu concentration (atoms per unit volume) in the bulk of the solder (far away from the boundary layer of the interface),  $c_s$  is the Cu saturation concentration in the solder, and  $k$  is a positive constant. According to Eq. (1), during dissolution, as more substrate atoms enter the molten solder,  $c$  increases and consequently  $dc/dt$  decreases with time. The maximum dissolution rate occurs when  $c$  approaches zero. This can take place either when time is very short or when the solder volume is very large. According to a recent study by Huang et al.,<sup>15</sup> the dissolution rate of a thin Cu foil (106 μm thick) dipped into a large amount (500 g) of Sn3.5Ag at 250 °C is quite high, reaching 8.7 μm/min. Because the

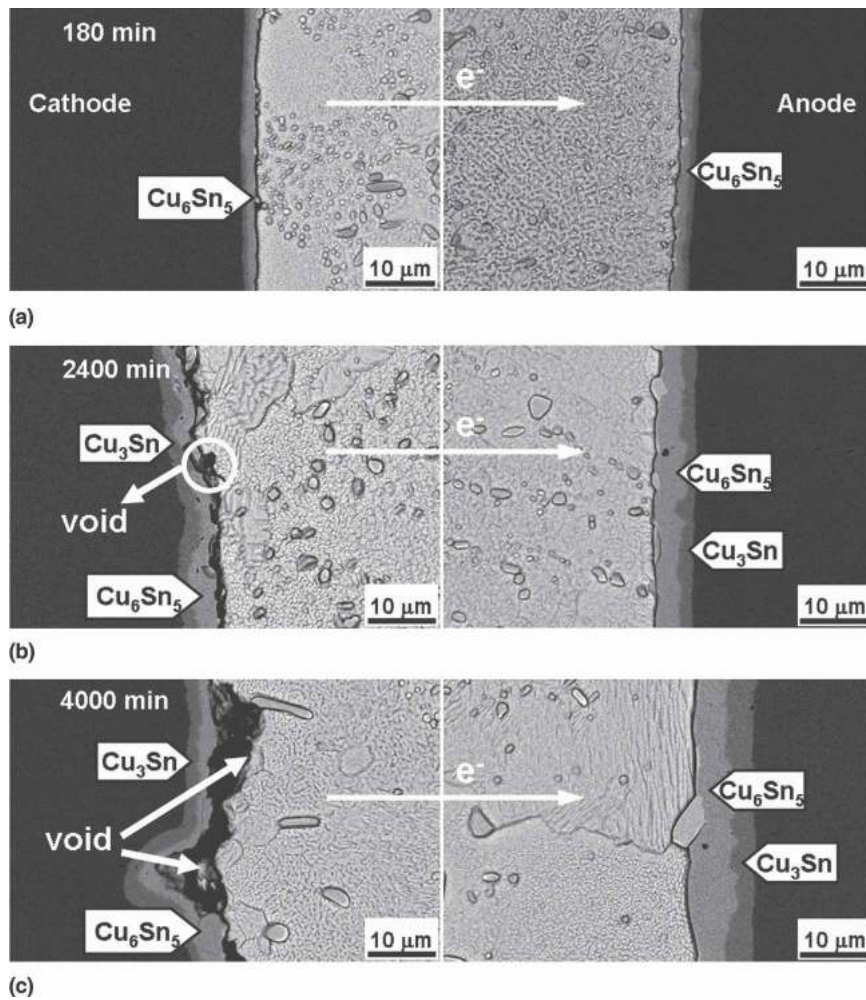


FIG. 6. Micrographs showing the sequence of events during current stressing at 200 °C, which is below the SnAg eutectic temperature at 221 °C. The current density through the solder was  $6.3 \times 10^3$  A/cm<sup>2</sup>, and the electrons flowed from the left side to the right: (a) after 180 min, (b) 2400 min, and (c) 4000 min of current stressing.

Cu foil was attacked by the solder on both surfaces, the single-side dissolution rate should then be 4.35 μm/min. The experimental conditions (a small piece of thin foil dipped into a very large amount of solder) used by Huang et al. approached the limit  $c \approx 0$ . In other words, the value 4.35 μm/min can be considered the maximum dissolution rate of Cu into Sn3.5Ag at 250 °C. As shown in Fig. 4, the initial dissolution rate, estimated by using linear extrapolation, was 1.3 μm/min when the electron current was applied. This value is below the maximum value of 4.35 μm/min. Therefore, one may conclude applying the current did not “accelerate” the dissolution beyond the maximum rate. It only somehow retained the high dissolution rate that the system would experience during the early stage of the dissolution. In other words, from Eq. (1), the applied current somehow reduced the value of  $c$  near the interface so the dissolution rate could remain high even though enough Cu atoms had entered the molten solder to make  $c$  approach  $c_s$ .

Before discussing how the applied current reduced the  $c$  value near the interface, we need to gain an idea of the value of  $c_s$  and the amount of dissolution needed to reach  $c_s$ . According to the binary Cu–Sn phase diagram,<sup>16</sup> the saturation solubility of Cu in Sn at 255 °C is  $\approx 1.6$  wt%. Assuming the Cu wires in Fig. 1 can dissolve only in the longitudinal direction, one can estimate to have the solder in Fig. 1 saturated with Cu at 255 °C, a total length of 9.2 μm has to be dissolved from the two Cu wires. The value was in qualitative agreement with the consumed thickness of the Cu wires for the case where no current was applied (see Fig. 4). Figure 4 shows that, at 30 min, 6 μm of Cu had been consumed on each Cu wire (for a total consumed thickness of  $2 \times 6 = 12$  μm) when no current was applied. After 30 min, the consumed thickness increased only very slightly. To sum up, if no current was applied, the solder became saturated with Cu very quickly ( $\approx 30$  min). Afterward, the dissolution rate approached zero according to Eq. (1). At this stage, the

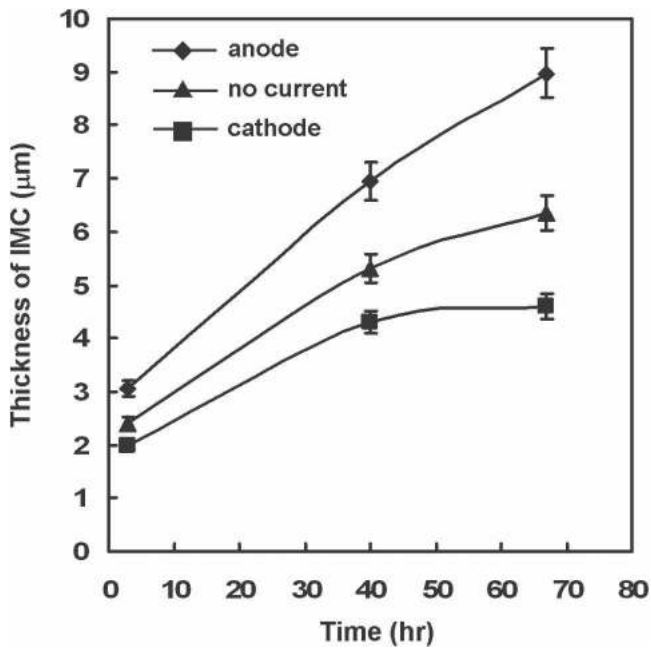


FIG. 7. Total thickness of the intermetallic compounds at the Cu/solder interfaces with and without applying current; temperature was 200 °C.

dissolution no longer played an important role in determining the consumption rate of the Cu. The Cu consumption rate now was dominated by the Cu–Sn chemical reaction, and the rate-limiting step was the interdiffusion of Cu and Sn through  $\text{Cu}_6\text{Sn}_5$  and  $\text{Cu}_3\text{Sn}$ , which was a relatively slow process.

The situation is different when the current was applied. The electron flow would drive the newly dissolved Cu atoms away from the cathode side toward the anode side. The electromigration Cu flux leaving the cathode side made the local Cu concentration near the cathode drop below the saturation so the dissolution of the Cu cathode could continue. On the other hand, the electromigration Cu flux arriving near the anode side would raise the local Cu concentration above the saturation limit, and as a result  $\text{Cu}_6\text{Sn}_5$  would precipitate near the anode side. In short, the Cu electromigration flux broke the otherwise local saturation equilibrium on the cathode side, making the local Cu concentration near the cathode drop below the saturation so that dissolution could continue. On the anode side, the arriving Cu flux also raised the local Cu concentration above the saturation limit, and so precipitation of  $\text{Cu}_6\text{Sn}_5$  occurred. This is why near the cathode Cu wire could continue dissolving and near the anode  $\text{Cu}_6\text{Sn}_5$  could continue precipitating. The fact the solder was undersaturated with Cu near the cathode side and supersaturated with Cu near the anode side suggested that a chemical potential gradient existed in the molten solder, with the Cu potential being higher on the anode side.

It is widely known that the electromigration flux in the solid-state is countered to a varied degree by the back stress flux. Liquid conducting media, however, cannot support any such back-stress, and as a result there is no back-stress flux to counter the electromigration flux. Nevertheless, in the present case electromigration in the liquid solder did set up a chemical potential gradient, and this chemical potential gradient in turn produced a countering flux. One can write the total atomic flux  $J_{\text{total}}$  as a summation of the electromigration flux  $J_{\text{em}}$  and the flux induced by the chemical potential gradient  $J_{\text{chemical}}$ :

$$J_{\text{total}} = J_{\text{em}} + J_{\text{chemical}} \quad , \quad (2)$$

$$= \frac{Dcz^*e\rho J}{kT} - D \frac{dc}{dx} \quad , \quad (3)$$

where  $D$  is the Cu diffusivity in molten solder,  $z^*$  is the effective charge of Cu,  $e$  is the charge of an electron,  $\rho$  is the resistivity of the solder,  $J$  is the electron current density,  $k$  is the Boltzmann constant,  $T$  is the absolute temperature, and  $x$  is the distance. Under the condition that the chemical potential flux exactly balances the electromigration flux,  $J_{\text{total}} = 0$ , and one obtains the following equation from Eq. (3):

$$z^*e\rho J = kT \frac{d \ln(c)}{dx} \quad . \quad (4)$$

The Cu chemical potential,  $\mu$ , is related to its concentration  $c$  through the following equation:

$$\mu = \mu^\circ + N^\circ kT \ln(\gamma c / \Omega) \quad , \quad (5)$$

where  $\mu^\circ$  is the standard-state chemical potential,  $N^\circ$  is Avogadro's number,  $\gamma$  is the activity coefficient, and  $\Omega$  is a conversion factor relating  $c$  to the Cu mol fraction ( $c/\Omega = \text{mol fraction}$ ). Because the Cu concentration is dilute, one can assume that both  $\gamma$  and  $\Omega$  can be taken as constants. Thus, one obtains the following equation from Eqs. (4) and (5):

$$\frac{d\mu}{dx} = N^\circ z^* e \rho J \quad . \quad (6)$$

Equation (6) represents the chemical potential gradient required to balance the electromigration flux. The distance from the Cu/Sn interface on the cathode side to the location where  $\text{Cu}_6\text{Sn}_5$  starts to precipitate,  $\Delta x$ , can be measured experimentally. The corresponding drop in the Cu chemical potential at these two locations,  $\Delta\mu$ , is difficult to measure or even interpret. If it is assumed that  $\Delta\mu$  is related to the supersaturation required for the  $\text{Cu}_6\text{Sn}_5$  precipitation to occur and is independent of the electron current density, then one can anticipate that  $\Delta x$  will decrease with increasing  $J$ . Additional experimental studies are required to verify this assumption.



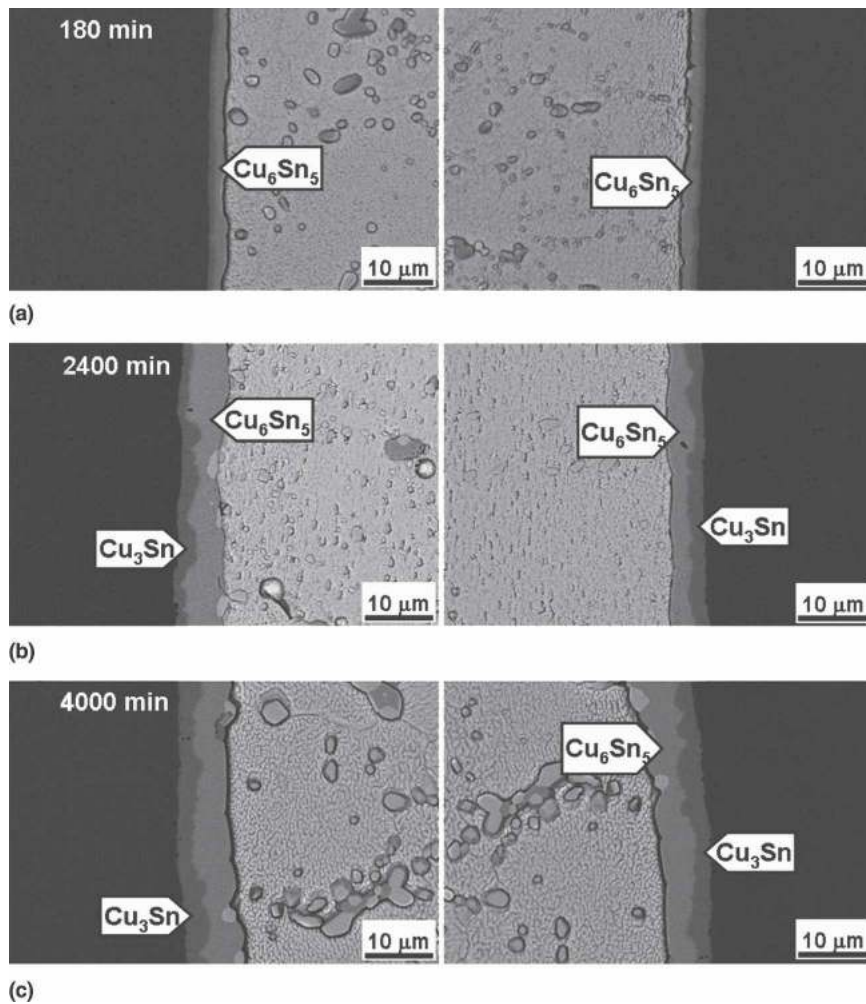


FIG. 8. Micrographs showing the two Cu/solder interfaces at 200 °C when no electron current was applied: (a) after 180 min, (b) 2400 min, and (c) 4000 min.

The analysis above is able to explain the trend shown in Fig. 4 that the consumption rate of the Cu cathode decreased as time increased, particularly at the later stage of the experiment. This trend can be understood by noting in Fig. 3 the length ( $\Delta x$ ) of the remaining solder between the Cu cathode and Cu<sub>6</sub>Sn<sub>5</sub> decreased with time. As  $\Delta x$  decreased, the absolute value of  $J_{\text{chemical}}$  increased according to Eq. (3). In other words,  $J_{\text{chemical}}$  was able to counter  $J_{\text{em}}$  flux to a greater and greater degree, and the net Cu flux  $J_{\text{total}}$  decreased, resulting in a smaller Cu consumption rate.

## V. SUMMARY

High electron current density caused the Cu cathode to dissolve at an accelerated rate, which was one order of magnitude greater than the no-current case. The dissolved Cu atoms were then driven by the electron current to the anode side and precipitated out as Cu<sub>6</sub>Sn<sub>5</sub>. Unlike electromigration in the solid state, there was no back-

stress flux to counter the electromigration flux in molten solder. There was, instead, a chemical potential flux to counter the electromigration. The chemical potential gradient,  $d\mu/dx$  required to balance the electromigration flux was derived to be  $d\mu/dx = N^{\circ}z^*e\rho J$ .

## ACKNOWLEDGMENT

The authors thank the National Science Council of Taiwan, Republic of China, for financial support through grants NSC-95-2221-E-002-441 and NSC-95-2811-E-008-004.

## REFERENCES

1. K.N. Tu: Recent advances on electromigration in very-large-scale integration of interconnects. *J. Appl. Phys.* **94**, 5451 (2003).
2. J.W. Nah, J.O. Suh, and K.N. Tu: Effect of current crowding and joule heating on electromigration induced failure in flip chip composite solder joints tested at room temperature. *J. Appl. Phys.* **98**, 013715 (2005).

3. L. Zhang, S. Ou, J. Huang, K.N. Tu, S. Gee, and L. Nguyen: Effect of current crowding on void propagation at the interface between intermetallic compound and solder in flip chip solder joints. *Appl. Phys. Lett.* **88**, 012106 (2006).
4. Y.H. Lin, Y.C. Hu, C.M. Tsai, C.R. Kao, and K.N. Tu: In-situ observation of the void formation and propagation mechanism in solder joints under current stressing. *Acta Mater.* **53**, 2029 (2005).
5. C.M. Tsai, Y.L. Lin, J.Y. Tsai, Y.S. Lai, and C.R. Kao: Local melting induced by electromigration in flip-chip solder joints. *J. Electron Mater.* **35**, 1005 (2006).
6. M.O. Alam, B.Y. Wu, Y.C. Chan, and K.N. Tu: High electric current density induced interfacial reactions in the micro-ball grid array ( $\mu$ BGA) solder joint. *Acta Mater.* **54**, 613 (2006).
7. Y.H. Lin, C.M. Tsai, Y.C. Hu, Y.L. Lin, and C.R. Kao: Electromigration induced failure in flip-chip solder joints. *J. Electron Mater.* **34**, 27 (2005).
8. Y.C. Hu, Y.H. Lin, and C.R. Kao: Electromigration failure in flip-chip solder joints due to rapid dissolution of copper. *J. Mater. Res.* **18**, 2544 (2003).
9. Y.H. Lin, C.M. Tsai, Y.L. Lin, J.Y. Tsai, and C.R. Kao: Electromigration induced metal dissolution in flip-chip solder joints. *Mater. Sci. Forum* **475–479**, 2655 (2005).
10. H.Y. Lu, H. Balkan, and K.Y.S. Ng: Solid–liquid reactions: The effect of Cu content on Sn–Ag–Cu interconnects. *JOM* **57**, 30 (2005).
11. T. Laurila, V. Vuorinen, and J.K. Kivilahti: Interfacial reactions between lead-free solders and common base materials. *Mater. Sci. Eng., R* **49**, 1 (2005).
12. A. Hayashi, C.R. Kao, and Y.A. Chang: Reactions of solid copper with pure liquid tin and liquid tin saturated with copper. *Scripta Mater.* **37**, 393 (1997).
13. H. Gan and K.N. Tu: Polarity effect of electromigration on kinetics of intermetallic compound formation in Pb-free solder v-groove samples. *J. Appl. Phys.* **97**, 063514 (2005).
14. V.I. Dybkov: *Growth Kinetics of Chemical Compound Layers* (Cambridge International Science, Cambridge, 1998), p. 135.
15. M.L. Huang, T. Loeher, A. Ostmann, and H. Reichl: Role of Cu in dissolution kinetics of Cu metallization in molten Sn-based solders. *Appl. Phys. Lett.* **86**, 181908 (2005).
16. Alloy phase diagrams, in *ASM Handbook*, Vol. 3, edited by H. Baker (ASM International, Materials Park, OH, 1992), pp. 2–178.